Article

Cell

A Vulnerability of a Subset of Colon Cancers with Potential Clinical Utility

Graphical Abstract

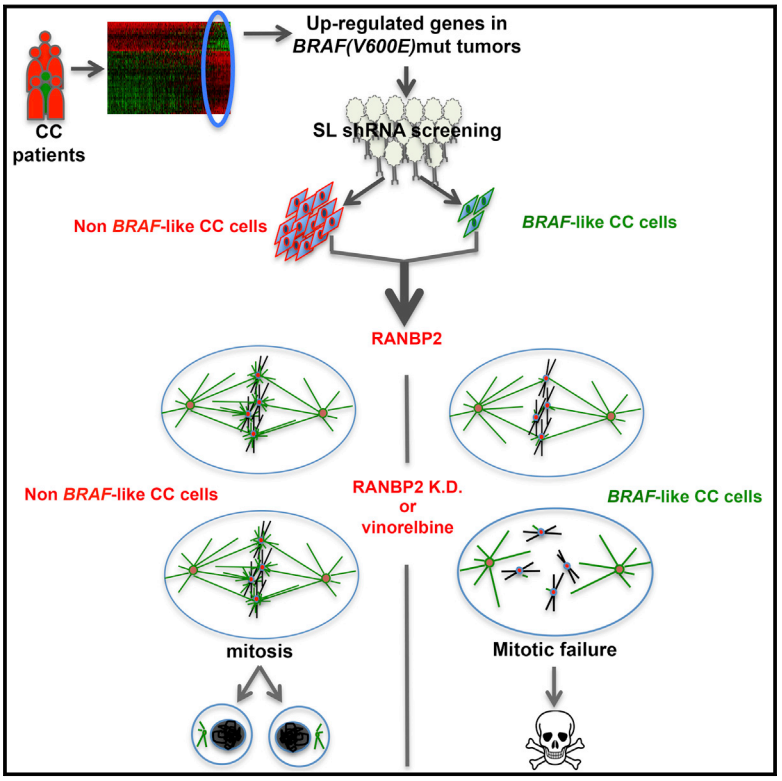

Authors

Loredana Vecchione, Valentina Gambino, Jonne Raaijmakers, ..., René H. Medema, Sabine Tejpar, René Bernards

Correspondence

r.bernards@nki.nl

In Brief

"BRAF-like" colorectal cancers, which are typically associated with poor patient outcome and resistance to conventional treatments, are selectively sensitive to the microtubule poison vinorelbine, suggesting that this subgroup of patients is likely to benefit from a tailored chemotherapy approach.

Highlights

- *RANBP2* loss is lethal to *BRAF*-like colon cancer (CC) cells
- *BRAF*-like CC cells have defective microtubule outgrowth from kinetochores
- RANBP2 loss exacerbates the defective microtubules outgrowth in BRAF-like CC cells
- Vinorelbine is selectively toxic to *BRAF*-like colon cancer cells

Vecchione et al., 2016, Cell *165*, 317–330
April 7, 2016
http://dx.doi.org/10.1016/j.cell.2016.02.059

CellPress

Cell

A Vulnerability of a Subset of Colon Cancers with Potential Clinical Utility

Loredana Vecchione,[1,16] Valentina Gambino,[1,16] Jonne Raaijmakers,[2] Andreas Schlicker,[1] Arianna Fumagalli,[3] Mariangela Russo,[4,5,6] Alberto Villanueva,[7] Evelyne Beerling,[3] Alice Bartolini,[5] David G. Mollevi,[7] Nizar El-Murr,[8] Marielle Chiron,[8] Loreley Calvet,[8] Céline Nicolazzi,[8] Cécile Combeau,[8] Christophe Henry,[8] Iris M. Simon,[9] Sun Tian,[9] Sjors in 't Veld,[9] Giovanni D'ario,[10] Sara Mainardi,[1] Roderick L. Beijersbergen,[1] Cor Lieftink,[1] Sabine Linn,[11] Cornelia Rumpf-Kienzl,[2] Mauro Delorenzi,[10,12,13] Lodewyk Wessels,[1] Ramon Salazar,[14] Federica Di Nicolantonio,[4,5] Alberto Bardelli,[4,5] Jacco van Rheenen,[3] René H. Medema,[2] Sabine Tejpar,[15] and René Bernards[1,*]

[1]Division of Molecular Carcinogenesis and Cancer Genomics Center Netherlands, The Netherlands Cancer Institute, Plesmanlaan 121, 1066 CX Amsterdam, the Netherlands

[2]Division of Cell Biology, The Netherlands Cancer Institute, Plesmanlaan 121, 1066 CX Amsterdam, the Netherlands

[3]Cancer Genomics Netherlands, Hubrecht Institute-KNAW and University Medical Center Utrecht, Uppsalalaan 8, 3584 CT Utrecht, the Netherlands

[4]Department of Oncology, University of Torino, SP 142, Km 3.95, 10060 Candiolo, Torino, Italy

[5]Candiolo Cancer Institute-FPO, IRCCS, SP142, Km 3.95, 10060 Candiolo, Torino, Italy

[6]FIRC Institute of Molecular Oncology (IFOM), 20139 Milano, Italy

[7]Program Against Cancer Therapeutic Resistance (ProCURE), Chemoresistance and Predictive Factors Group, Catalan Institute of Oncology (ICO) and Bellvitge Institute for Biomedical Research (IDIBELL), L'Hospitalet del Llobregat, 08908 Barcelona, Spain

[8]Sanofi Oncology, 13 Quai Jules Guesde, 94403 Vitry sur Seine, France

[9]Agendia, Science Park 406, 1098 XH Amsterdam, the Netherlands

[10]Bioinformatics Core Facility, SIB Swiss Institute of Bioinformatics, Quartier Sorge - Batiment Genopode, 1015 Lausanne, Switzerland

[11]Division of Molecular Pathology, The Netherlands Cancer Institute, Plesmanlaan 121, 1066 CX Amsterdam, the Netherlands

[12]Department of Oncology, University of Lausanne, Rue de Bugnon 21, 1011 Lausanne, Switzerland

[13]Ludwig Center for Cancer Research, University of Lausanne, Chemin des Boveresses 155, 1066 Epalinges, Switzerland

[14]Medical Oncology Department, Catalan Institute of Oncology, IDIBELL, Bellvitge Biomedical Research Institute, L'Hospitalet de Llobregat, 08908 Catalonia, Spain

[15]Molecular Digestive Oncology, University Hospitals Leuven and KU Leuven, Herestraat 49, 3000 Leuven, Belgium

[16]Co-first author

*Correspondence: r.bernards@nki.nl

http://dx.doi.org/10.1016/j.cell.2016.02.059

SUMMARY

BRAF(V600E) mutant colon cancers (CCs) have a characteristic gene expression signature that is also found in some tumors lacking this mutation. Collectively, they are referred to as "*BRAF*-like" tumors and represent some 20% of CCs. We used a shRNA-based genetic screen focused on genes upregulated in *BRAF(V600E)* CCs to identify vulnerabilities of this tumor subtype that might be exploited therapeutically. Here, we identify RANBP2 (also known as NUP358) as essential for survival of *BRAF*-like, but not for non-*BRAF*-like, CC cells. Suppression of RANBP2 results in mitotic defects only in *BRAF*-like CC cells, leading to cell death. Mechanistically, RANBP2 silencing reduces microtubule outgrowth from the kinetochores, thereby inducing spindle perturbations, providing an explanation for the observed mitotic defects. We find that *BRAF*-like CCs display far greater sensitivity to the microtubule poison vinorelbine both in vitro and in vivo, suggesting that vinorelbine is a potential tailored treatment for *BRAF*-like CCs.

INTRODUCTION

Colorectal cancer (CRC) represents one of the most common cancers worldwide, with an estimated 1.2 million cases yearly and an annual mortality of over 600,000 (Jemal et al., 2011). Due to the relatively asymptomatic progression of the disease in the early stages, patients are frequently diagnosed with metastatic disease, with a five-year survival rate of around 10% (Cidón, 2010). BRAF is a protein kinase downstream of RAS in the RAS-RAF-MEK-ERK kinase pathway. V600E is the most common point mutation of the *BRAF* gene and is present in approximately 8%–10% of the CRC patients (Tie et al., 2011; Yuan et al., 2013). Several reports have consistently shown the negative impact of *BRAF(V600E)* mutation on CRC prognosis, especially in the metastatic setting (Bokemeyer et al., 2011; Van Cutsem et al., 2011; Richman et al., 2009; Tol et al., 2009). *BRAF(V600E)* colon cancers (CCs) are characterized by a distinct and homogeneous gene expression profile when compared to *KRAS* mutant and *KRAS-BRAF* double wild-type (WT2) CCs. (Popovici et al., 2012; Tian et al., 2013). This *BRAF* mutant gene expression signature identifies *BRAF* mutant tumors with high sensitivity (96%), and when applied to *BRAF* WT CCs, it also identifies subsets of *KRAS* mutant (30%) and a subset of WT2 (13%) tumors. Tumors having this gene signature are referred to as "*BRAF*-like" and have a similar poor prognosis

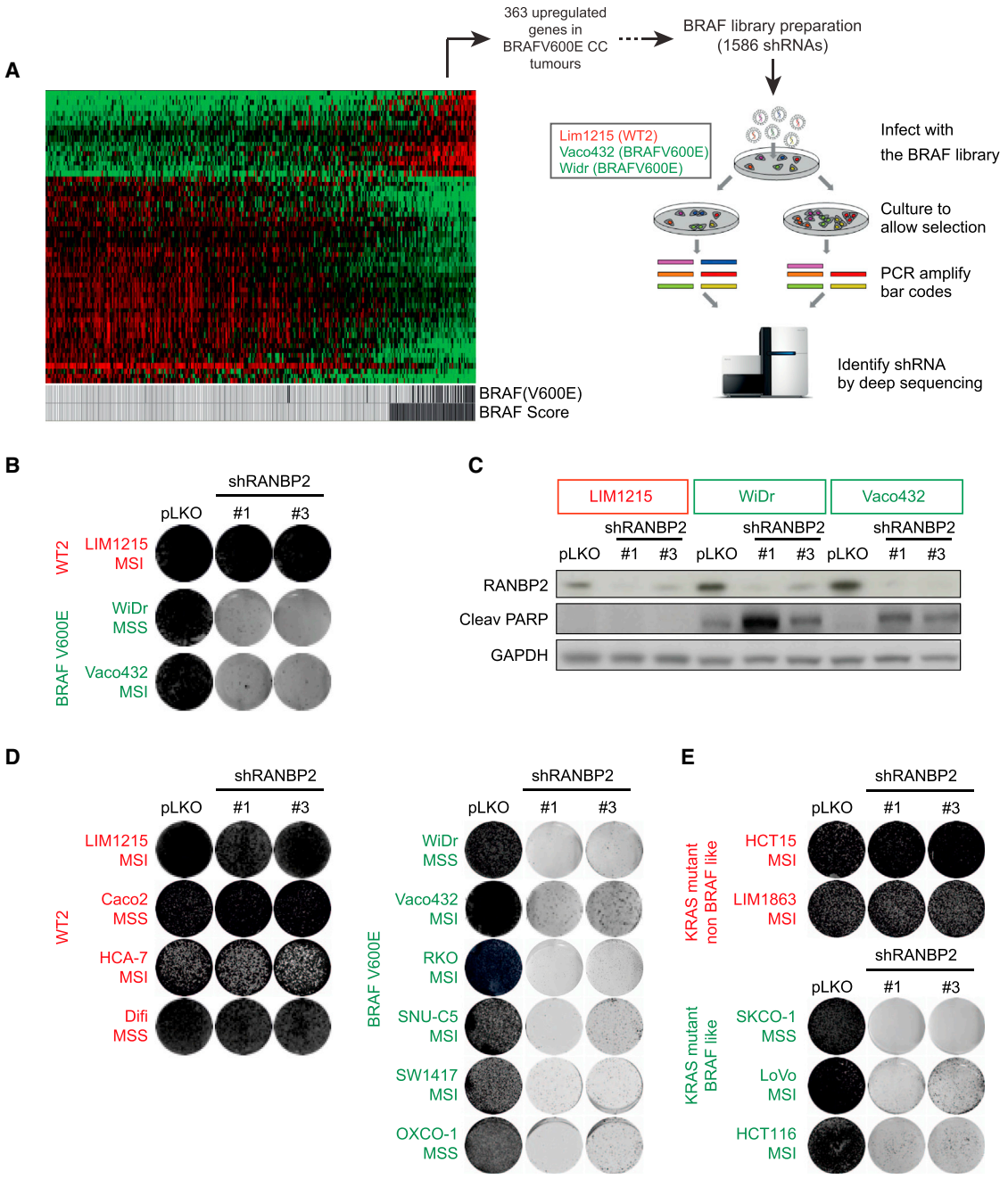

Figure 1. Identification and Validation of *RANBP2* Synthetic Lethality with *BRAF*-like Phenotype in Colon Cancer

(A) *BRAF(V600E)*-specific upregulated genes are used to assemble the BRAF library and perform a "dropout" shRNA screening. Left panel: example of a heatmap of BRAF activating a 58-gene signature across 381 colon tumor samples of one of the two datasets considered (Tian et al. 2013). Tumors are sorted according to the signature scores. Upper row: tumors with BRAF(V600E) oncogenic mutations as measured by sequence analysis are indicated by the black boxes, and tumors without BRAF(V600E) oncogenic mutations are indicated by the white boxes. Lower row: tumors sharing the gene expression pattern of BRAF oncogenic mutation as measured by the signature are displayed as black boxes (BRAF-like subgroup), and tumors that share the gene expression pattern of BRAF-wild-type are displayed as white boxes. The BRAF-like subgroup includes tumors with V600E mutation, tumors with KRAS mutation, and tumors wild-type for KRAS and BRAF. Right panel: a schematic outline of the "dropout" shRNA screen for genes whose inhibition is selectively lethal in *BRAF*-like CC cell lines. After selecting 363 upregulated genes in BRAF(V600E) CCs tumors from the two datasets, the BRAF library was generated. Two *BRAF(V600E)* CC cell lines, Vaco432 and WiDr, were infected with the BRAF shRNA library polyclonal virus and screened for shRNAs that cause lethality. LIM1215 CC cell line (WT2) was used as a control.

(B, D, and E) RANBP2 is synthetically lethal with *BRAF*-like phenotype in CC cells. WT2 CC cells (LIM1215, Caco2, HCA7, and Difi), *BRAF(V600E)* CC cells (WiDr, Vaco432, RKO, SNU-C5, SW1417, and OXCO-1), *KRAS* mutant non-*BRAF*-like CC cells (HCT15 and LIM1863), and *KRAS* mutant *BRAF*-like CC cells (SKCO-1,

(legend continued on next page)

regardless of the presence of the *BRAF(V600E)* mutation. The treatment of both early-stage and metastatic cancer patients is mainly based on chemotherapy. Predictive biomarkers of response are required to help identify the group of patients who might benefit from certain chemotherapeutic treatments and avoid unnecessary toxicity for those who will not benefit. To date, very few predictive biomarkers for chemotherapy response have been identified and none of them are used in clinical practice (Glück et al., 2013; Roepman et al., 2014; Sargent, 2014; Sinicrope et al., 2011; Vollebergh et al., 2014).

Functional genetic screens represent a powerful tool to identify mechanisms of drug response and synthetic lethal interactions (Berns et al., 2007; Luo et al., 2009; Prahallad et al., 2012; Steckel et al., 2012). We applied a loss-of-function genetic screen to identify vulnerabilities of *BRAF*-like colon cancer cells. Here, we describe a specific Achilles heel of these cells that can be targeted by vinorelbine, a chemotherapeutic drug currently not used clinically for the treatment of colon cancer.

RESULTS

RANBP2 Suppression Is Selectively Lethal to *BRAF*-like Colon Cancers

To identify synthetic lethal interactions of *BRAF* mutant colon cancer, we performed a loss-of-function genetic screen in which we specifically focused on genes upregulated in *BRAF(V600E)* CCs. We hypothesized that some of these genes may be selectively required to tolerate the presence of the *BRAF* mutation. We identified 363 genes that are overexpressed in *BRAF* mutant CCs as compared to *BRAF* and *KRAS* wild-type (*WT2)* CCs using two gene expression datasets (Popovici et al., 2012; Tian et al., 2013) (Figure 1A, left). For each dataset, the genes overexpressed in *BRAF* mutant tumors were determined, using a cutoff of 0.05 on the Benjamini-Hochberg false discovery rate to control for multiple testing. We selected 163 genes common to both datasets, as well as the top 100 of the remaining upregulated genes unique to each dataset, yielding in total a set of 363 genes. The individual lists of genes are reported in Table S1. We then selected 1,586 short hairpin RNA (shRNA) vectors from the TRC shRNA collection (TRC-Hs1.0) to generate a sub-library targeting the 363 genes of interest (''BRAF library''). To identify those genes that are specifically lethal in *BRAF*(V600E) cells versus WT2 cells, we selected three CC cell lines. WiDr and Vaco432 colon cancer cell lines harbor a *BRAF(V600E)* gene mutation and are defined as *BRAF*-like by gene expression signature. The LIM1215 colon cancer cell line is wild-type for *KRAS* and *BRAF* genes (WT2) and is defined as non-*BRAF*-like by signature.

WiDr, Vaco432, and LIM1215 were infected with the BRAF shRNA library. The infected cells were selected for viral integration and cultured for 13 days, after which time shRNAs were recovered by PCR (Figure 1A, right). The relative abundance of shRNA vectors was determined by next-generation sequencing of the barcode identifiers present in each shRNA vector (Table S2). We first considered shRNA vectors that were significantly depleted in *BRAF(V600E)* CC cells at day 13 as compared to day 0 by at least 50% (log2 time13/time0 ≤ -1, p adjusted value ≤ 0.1). Subsequently, we determined the fold depletion between *BRAF* mutant CC cells and LIM1215 cells and selected those shRNAs that had a ratio of more than 2-fold (WM fold change ≥ 2). To increase the fidelity of the hits, genes represented by multiple shRNAs matching these criteria were prioritized (Table S3). From this list we selected *RANBP2* represented by three individual shRNAs for further validation and follow-up. We tested all five *RANBP2* shRNAs present in the library in *BRAF(V600E)* cells and WT2 cells and confirmed the increased sensitivity of the *BRAF(V600E)* CC cells upon RANBP2 silencing as compared to WT2 CC cells (Figures S1A and S1B). Based on their knockdown efficiency, shRNAs #1 and #3 were selected for further studies. In a second independent experiment, colony formation assays confirmed that silencing of *RANBP2* with shRNA#1 and #3 specifically impaired the proliferation of the two *BRAF* mutant (Vaco432 and WiDr) CC cell lines, but not the WT2 CC cell line LIM1215 (Figure 1B). This impairment correlated with cell death as shown by increased apoptosis (Figure 1C).

Since the genes tested in this genetic screen are not only upregulated in *BRAF* mutant CCs but also in the *BRAF*-like CCs, we also studied *RANBP2* suppression as a potential vulnerability in a larger panel of CC cell lines that are either *BRAF*-like or non-*BRAF*-like by gene signature. Cell lines were categorized as WT2, *BRAF(V600E)* , or *KRAS* mutant based on mutation status and, based on gene expression, as *BRAF*-like or non-*BRAF* like. The proliferation of none of the six non-*BRAF*-like CC cell lines was impaired by *RANBP2* suppression, regardless of *KRAS* mutation status. In contrast, proliferation of all nine *BRAF*-like CC cell lines was dramatically inhibited upon *RANBP2* suppression, regardless of *KRAS* and *BRAF* mutation status (Figures 1D and 1E). Microsatellite instability (MSI) status did not correlate with this phenotype either. The degree of *RANBP2* silencing is comparable across the different cell lines (Figure S1C). The sensitivity observed in BRAF-like cells is related to the silencing of the gene rather than to an unspecific effect of the hairpins since no toxicity was observed, either with scrambled RANBP2 shRNA or with pLKO as compared to parental lines (Figure S1D). We conclude that *RANBP2* knockdown is selectively lethal for *BRAF*-like CC cell lines.

RANBP2 Knockdown Causes Mitotic Abnormalities in *BRAF*-like Cells

RANBP2 is a small GTP-binding protein belonging to the RAS superfamily and, as part of the nuclear pore complex, is a crucial regulator of nucleo-cytoplasmic transport. However, it also plays an important yet ill-defined role in kinetochore function during mitosis. RANBP2 silencing has been reported to be responsible

LoVo, and HCT116) were stably infected with two independent shRNAs targeting *RANBP2* (sh*RANBP2* #1 and sh*RANBP2* #3). Viability was assessed by a colony formation assay. The pLKO vector was used as a control. Cells were fixed, stained, and photographed after 10 days of culture.
(C) The level of knockdown of RANBP2 protein and apoptosis induction was measured by western blot.
See also Figure S1 and Tables S1, S2, and S3.

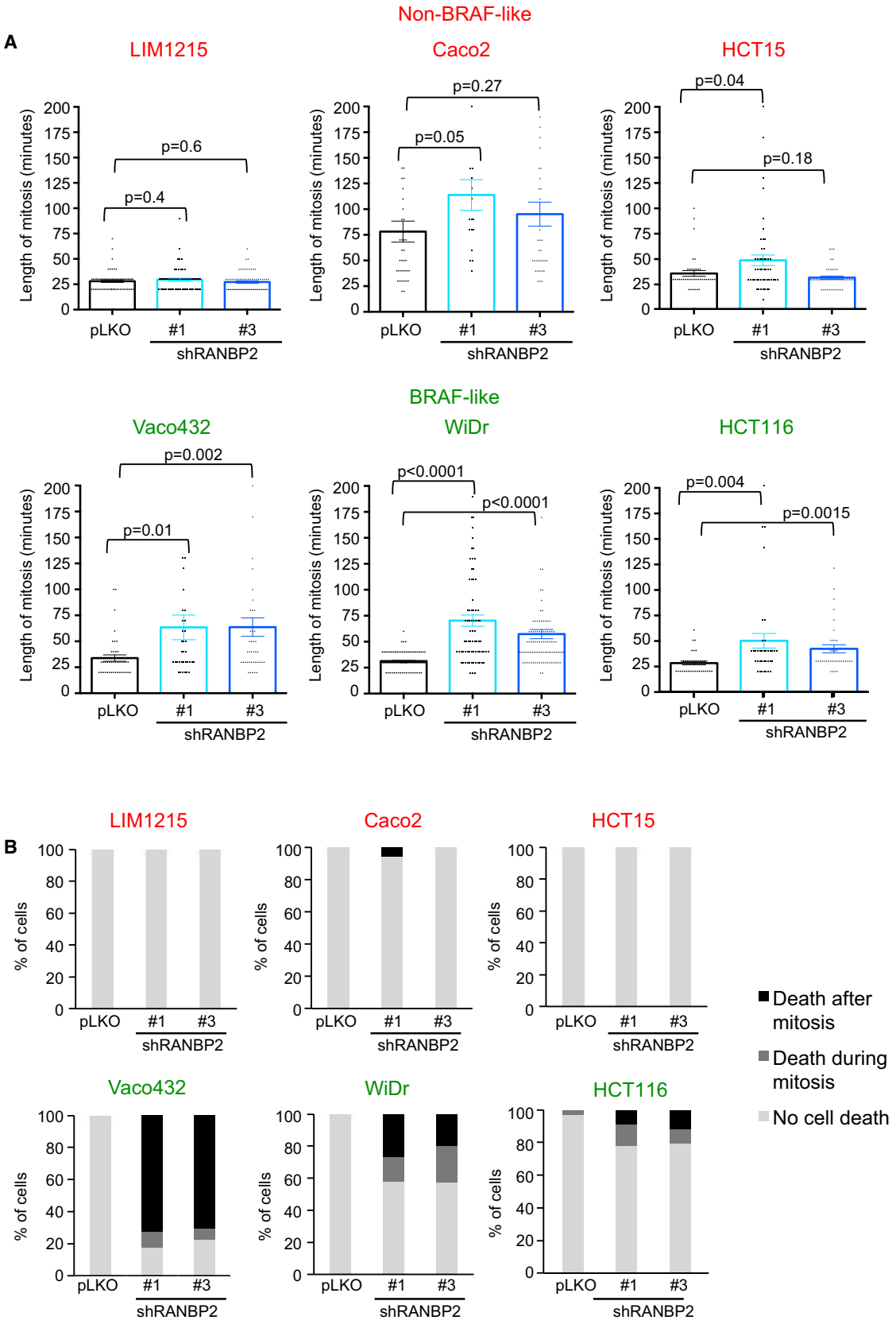

(legend on next page)

for abnormal mitotic progression and abnormal chromosome segregation, eventually leading to mitotic catastrophe (Hashizume et al., 2013; Salina et al., 2003). We therefore asked whether *RANBP2* expression in *BRAF*-like colon cancer cells is required for mitotic progression. We performed time-lapse microscopy experiments in three different non-*BRAF*-like CC cells (LIM1215, Caco2, and HCT15) and three different *BRAF*-like CC cells (Vaco432, WiDr, and HCT116) upon RANBP2 silencing. Cells were first transduced with GFP-tagged histone H2B (H2B-GFP) to allow visualization of the chromosomes in mitosis and then infected with RANBP2 shRNA #1 or #3 or control vector pLKO. Images were acquired every 10 min over a period of 72 hr. The degree of *RANBP2* silencing is shown in Figure S2A. Figure 2A shows that for *BRAF*-like CC cells silencing of *RANBP2* resulted in a significant increase of the time spent in mitosis (two times longer) as compared to pLKO-infected cells. In contrast, length of mitosis was only slightly increased (0.8 to 1.4 times longer) in non-*BRAF*-like CC cells upon *RANBP2* loss. Moreover, up to 75% of the mitotic events counted in *BRAF*-like *RANBP2*-depleted CC cells displayed a range of defects, including delay in alignment, metaphase delay, spindle defects, anaphase bridges, and lagging chromosomes (Figure S2B). These abnormalities eventually lead to death during or straight after mitosis (Figure 2B). In contrast only few mitotic defects (2% in LIM1215, 4% in HCT15, and 6% in Caco2, respectively) were observed in non-*BRAF*-like CC cells. These results show that *RANBP2* suppression induced cell death in *BRAF*-like CC cells is driven by defects in mitosis and identifies mitosis as a potential vulnerability of *BRAF*-like CC cell lines.

RANBP2 Knockdown Affects Microtubule Dynamics in *BRAF*-like Cell Lines

RANBP2 is part of the RANBP2-RANGAP1 complex. It has been shown to play a role in the interaction of kinetochores with kinetochore fibers and in regulating the function of kinetochores through its cyclophilin-like domain and E3 SUMO-ligase domain (Arnaoutov et al., 2005; Clarke, 2005). It was hypothesized that the interaction of the RANBP2-RANGAP1 complex with kinetochores can also regulate other effectors through localized GTP hydrolysis by RAN (Clarke and Zhang, 2008). RAN-regulated targets in mitosis include mostly microtubule-stabilizing factors and factors involved in microtubule nucleation (Clarke and Zhang, 2008). We also observed several mitotic defects in *BRAF*-like CC cells upon *RANBP2* suppression, including spindle defects. To better evaluate whether any abnormalities in the microtubule (MT) nucleation could explain the essential mitotic role of RANBP2 in *BRAF*-like CC, we performed nocodazole washout experiments, a standard tool to study MT outgrowth from centrosomes and kinetochores. We first disassembled MTs by using high-dose nocodazole for a short time period, and after removal of the drug, the initial stage of MT regrowth at both centrosomes and kinetochores was evaluated in a time-course analysis. The first experiment was performed in a non-*BRAF*-like CC cell line (Caco2) and in a *BRAF*-like CC cell line (WiDr). Within 30 min of nocodazole removal both the non-*BRAF*-like CC cell line (Caco2) and the *BRAF*-like CC cell line (WiDr) showed an almost mature spindle, thus indicating the reversible action of the drug (Figures 3A and 3B). A robust microtubule growth from both centrosomes and kinetochores was observed in the non-*BRAF*-like CC cell line (Figure 3A), while a severe impairment of microtubule growth from kinetochores was observed in the *BRAF*-like CC cell line within the first 6 min of the time course (Figure 3B). To further characterize the robustness of this phenotype, we performed nocodazole washout experiments in several CC cell lines previously categorized based on the *BRAF*-like status. As shown in Figure 3C, we did not observe any major differences in terms of MTs outgrowth from the centrosomes between *BRAF*-like and non-*BRAF*-like CC cells within the first 6 min of the time course. However, we observed a clear impairment of microtubule outgrowth from the kinetochores in *BRAF*-like CC cells compared to non-*BRAF*-like CC cells (Figure 3D) in the same time frame. Sample images for the categories used to score the outgrowth from both the centrosomes and the kinetochores are reported in Figure S3A. Nucleation of MTs from kinetochores is regulated by the RAN gradient, as well by the RANGAP1-RANBP2 complex (Clarke and Zhang, 2008; Torosantucci et al., 2008). The impairment of MTs outgrowth from the kinetochores observed in *BRAF*-like CC cells could explain their dependency on RANBP2. We therefore asked what the role of RANBP2 is in MTs nucleation from the kinetochores in *BRAF*-like and non-*BRAF*-like CC. Two non-*BRAF*-like (Caco2 and HCT15) and two *BRAF*-like (WiDr and HCT116) CC cell lines were infected with the RANBP2 shRNAs #1 or #3 and pLKO as a control. After puromycin selection, cells were harvested and seeded for a nocodazole washout experiment. Three independent biological replicates were performed per cell line, and the MTs outgrowth from both the centrosomes and the kinetochores was again scored within the first 6 min of nocodazole washout by using the same scoring methodology as described for Figures 3C and 3D. We considered the two cell lines in each group to belong to the same category. To increase statistical power, we combined the results of the three independent replicate measurements of the two cell lines in each group. As shown in Figure 3E, neither the MTs outgrowth from the centrosomes nor

Figure 2. *RANBP2* Knockdown Affects Mitosis and Induces Cell Death Selectively in *BRAF*-like CC Cell Lines

(A) *RANBP2* knockdown increases mitosis length in *BRAF*-like CC cells. H2B-GFP non-*BRAF*-like CC cells (LIM1215, Caco2, and HCT15) and H2B-GFP BRAF-like CC cells (Vaco432, WiDr, and HCT116) were stably infected with two different shRNAs targeting *RANBP2* (shRANBP2#1 and shRANBP2#3) and observed by time-lapse microscopy. For each CC cell line, pLKO was used as a negative control. The length (A) and the faith of mitosis (B) were assessed. Data are represented as mean ± SEM. The p value was calculated versus the pLKO-infected group (unpaired t test with equal SD). The average number of mitosis evaluated per condition was 50.

(B) *RANBP2* knockdown induces death during or directly after mitosis selectively in *BRAF*-like CC cells. A graphic representation of cellular death quantification occurring during mitosis or immediately after mitosis (within 3 hr from cytokinesis) is shown. The y axis indicates the percentage of cells showing no cell death, death during mitosis, and death after mitosis.

See also Figure S2.

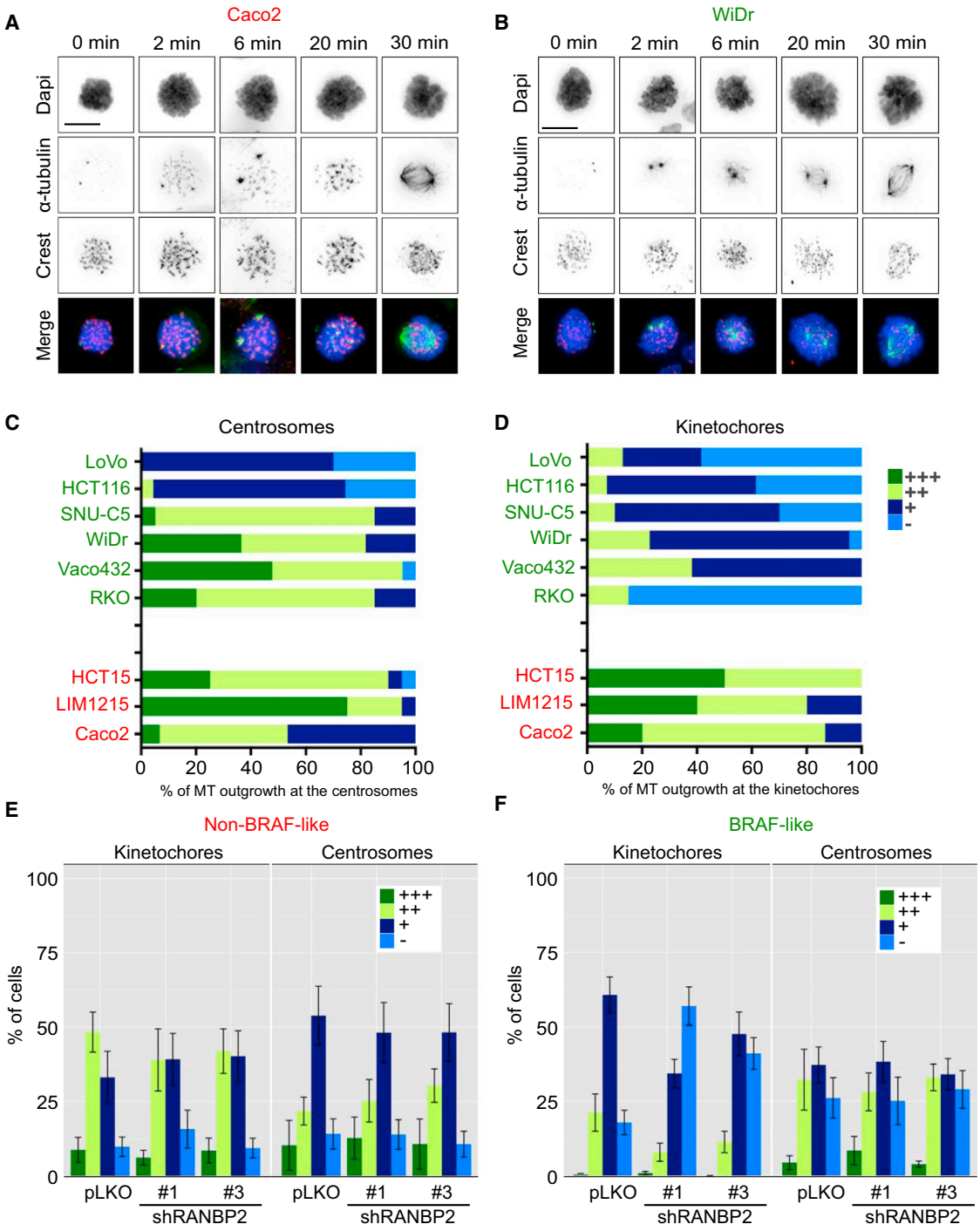

Figure 3. *BRAF*-like CC Cells Have Less Microtubule Nucleation from Kinetochores that Is Further Reduced by *RANBP2* Knockdown

(A and B) Representative images of MT outgrowth after nocodazole washout in Caco2 (non-BRAF-like CC cell line) and WiDr (BRAF-like CC cell line). Scale bars indicate 10 μm. Cells were stained for α-tubulin to visualize MTs, CREST to visualize the kinetochores, and DAPI to visualize DNA. See the Supplemental Experimental Procedures for details.

(C and D) Quantification of microtubule outgrowth at the centrosomes (C) or at the kinetochores (D) in non-*BRAF*-like (Lim1215, Caco2, and HCT15) and *BRAF*-like CC cell lines (RKO, Vaco432, WiDr, SNU-C5, HCT116, and LoVo). The y axis indicates the two groups of cells, and the x axis indicates the percentage of cells showing no ("−"), weak ("+"), medium ("++"), or strong ("+++") microtubule outgrowth.

(legend continued on next page)

the MT outgrowth from the kinetochores was perturbed in non-*BRAF*-like cell lines upon *RANBP2* knockdown. Interestingly, we found that *RANBP2* knockdown significantly decreased MTs outgrowth from the kinetochores in *BRAF*-like CC cell lines, as evidenced by the reduction of the "weak outgrowth" category ("+") and the increase of the "null outgrowth" category ("−"). In particular, the weak outgrowth category dropped from 61% in controls to 34% with shRNA #1 (Benjamini-Hochberg false discovery rate [FDR = 0.08]) and to 48% with shRNA #3 (FDR = 0.5). The null outgrowth category increased from 18% in the pLKO condition to 57% with hairpin #1 (FDR = 0.003) and to 41% with hairpin #3 (FDR = 0.02). The analysis for the individual cell lines with the corresponding silencing is shown in Figures S3B–S3F. These results show that silencing of *RANBP2* further reduces MT nucleation from the kinetochores, suggesting that *BRAF*-like CC tumors rely on *RANBP2* to compensate for an impairment of MTs nucleation from the kinetochores. This makes these tumors particularly vulnerable to loss of *RANBP2* expression. Indeed, its loss triggers spindle perturbations that cause several mitotic defects, leading to cell death.

BRAF-like Colon Cancer Cells Are Sensitive to Vinorelbine

We found that *RANBP2* loss perturbs spindle formation, prolongs the time spent in mitosis, triggers several mitotic defects, and, ultimately, induces death during or immediately after mitosis, which raises the possibility that *BRAF*-like CC cells are vulnerable to mitotic spindle poisons that act on microtubule dynamics. To address this, we mined the data from the Genomics of Drug Sensitivity in Cancer project (Sanger panel) to see if *BRAF(V600E)* CC cell lines are more sensitive to mitotic drugs as compared to WT2 CC cell lines (Garnett et al., 2012). Data were available for a total of 15 CC cell lines that were tested for sensitivity to both vinca alkaloid compounds (vinorelbine and vinblastine) and taxanes (paclitaxel and docetaxel). As shown in Figure 4A, no significant difference in sensitivity was observed for vinblastine (Wilcoxon test p value = 0.85), paclitaxel (p value = 0.13), and docetaxel (p value = 0.2). *BRAF(V600E)* CC lines, however, were significantly more sensitive to vinorelbine than WT2 CC cells (p value = 0.04) with a difference of over 30-fold in the median IC_{50} values. To further validate these findings we treated a panel of 22 colon cancer cell lines for 72 hr with different concentrations of vinorelbine, vinblastine, and paclitaxel. Our cell lines were previously profiled for gene expression to define their BRAF-like status and were homogeneously distributed among the two categories (11 BRAF-like and 11 non-BRAF-like cell lines). As reported in Figure 4B, we also observed a significant difference in sensitivity to vinblastine and paclitaxel in BRAF-like cells as compared to non BRAF-like cells, in contrast with what was observed in the Sanger panel. This could be explained by the relatively small number of cells tested in the Sanger panel. Despite its statistical significance, the difference observed in the median IC_{50} values for paclitaxel is only about 2-fold, while for vinorelbine and vinblastine it is more than 100-fold (Table S4).

To corroborate the sensitivity of BRAF-like CC cells to the vinca alkaloid compounds, we treated the same panel of CC cell lines with vinorelbine, vinblastine, and paclitaxel for about 2 weeks in colony formation assays. Figures 4C–4F shows that the lethal concentration of vinorelbine for non-BRAF-like CC cells ranged between 10 and >100 nM, while BRAF-like CC cells showed a lethal dose ranging between 0.01 and 1 nM. This means that *BRAF*-like CC cells were 10- to 10,000-fold more sensitive to vinorelbine compared to non-BRAF-like. The differences observed with paclitaxel were more limited (about 2-fold; data not shown), while vinblastine showed a difference of 10- to 100-fold (Figures S4A and S4B). These results confirmed the specific vulnerability of *BRAF*-like CC cell lines to vinorelbine as also observed in the Sanger cell line dataset and in our short-term assays. The exquisite sensitivity of *BRAF*-like CC cells lines to vinorelbine was not related to an increased proliferation rate since the proliferation rate of *BRAF*-like CC cell lines was not significantly different from that of non-*BRAF*-like cell lines (Figure S4C). Importantly, *BRAF(V600E)* CC cells lines had an IC_{50} for vinorelbine that was similar to that of breast and lung cancer cell lines, two solid tumors for which vinorelbine is used in clinical practice (Figure S4D).

To further characterize the vulnerability of *BRAF*-like CC to vinorelbine, H2B-YFP-expressing CC cells were analyzed by time-lapse microscopy upon vinorelbine treatment (10 nM) over 72 hr. As reported in Figure 4G, while non-BRAF-like CC cells were dividing over a period of 24 hr of observation upon vinorelbine treatment, *BRAF*-like CC cells were mainly arrested in mitosis, with a percentage of cells dying during mitosis or slipping out of mitosis followed by cell death. After 72 hr of vinorelbine treatment, non-BRAF-like CC cells were still dividing with a minor percentage of cells dying and slipping out of mitosis, while *BRAF*-like CC were mainly dead with a minor percentage of cells still arrested in mitosis (Figure 4H). These findings were further confirmed by western blot analysis. We observed an arrest in M phase with an increase of the cyclin B1 levels after 24–48 hr of treatment and in some cases after 12 hr, followed by apoptosis in *BRAF*-like CC cells (Figure S4E), while we only observed a slight increase of cyclin B1 with mild apoptosis in HCT15 (non-BRAF-like) and a slight increase of apoptosis in LIM1215 (non-BRAF-like) over a 72-hr treatment.

In Vivo Effects of Vinorelbine

To assess whether the in vitro findings can be recapitulated in vivo, Vaco432 and RKO (*BRAF*(*V600E*) BRAF-like), HCT116 (*KRAS* mutant BRAF-like), SW480, and HCT15 (*KRAS* mutated non-*BRAF*-like) CC cells were injected in nude mice. Upon tumor establishment (200–250 mm^3), xenografts were treated with either vehicle or vinorelbine (10 mg/kg) for 40–50 days.

(E and F) Quantification of microtubule outgrowth from kinetochores or centrosomes in non-*BRAF*-like (E) (Caco2 and HCT15) and *BRAF*-like cell lines (F) (WiDr and HCT116) upon *RANBP2*^{KD}. The y axis indicates the percentage of cells showing no ("−"), weak ("+"), medium ("++"), or strong ("+++") microtubule outgrowth. Error bars represent SEM. The x axis reports the three different conditions, pLKO and RANBP2^{KD} cells (both shRNAs #1 and #3). Each experiment was performed in triplicates, and both the scoring and the analysis were performed blinded.
See also Figure S3.

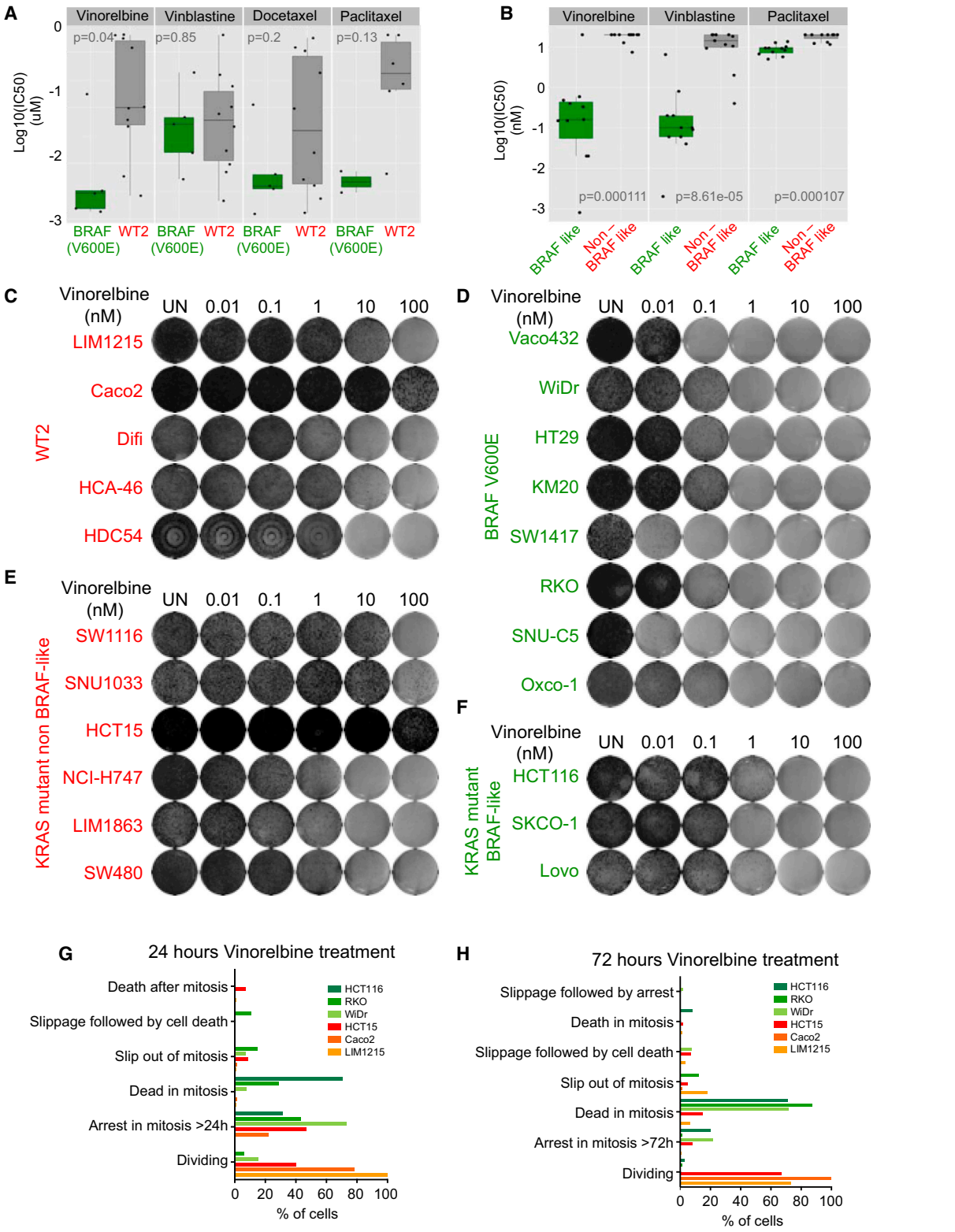

Figure 4. Vinorelbine Selectively Kills *BRAF*-like CC Cell Lines

(A) Boxplot of $\log_{10}$ IC_{50} values for treatment of *BRAF(V600E)* and WT2 CC cell lines with vinorelbine (10 WT2 and 5 BRAF(V600E) cells), vinblastine (10 WT2 and 4 BRAF(V600E) cells), docetaxel (10 WT2 and 5 BRAF(V600E) cells), and paclitaxel (6 WT2 and 2 BRAF(V600E) cells) extracted from the Genomics of Drug Sensitivity in Cancer project. $\log_{10}$ of IC_{50} values (μM) are shown.

(legend continued on next page)

Vinorelbine treatment significantly impaired tumor growth of *BRAF*-mutated (Vaco432) and *BRAF*-like (HCT116) xenografts, while no antitumor effect was observed in non-*BRAF*-like (SW480 and HCT15) mice (Figures 5A–5D). While RKO cells were very sensitive to vinorelbine in vitro (Figure 4D) and to RANBP2 silencing (Figure S5A), no effect was observed in RKO xenografts (Figure 5E). This suggests that the drug response in vivo can be modulated by factors from the local microenvironment. In particular, TGFβ can lead to powerful resistance to a number of cancer drugs, including chemotherapy (Brunen et al., 2013; Huang et al., 2012). To test whether RKO cells are sensitive to TGFβ-induced drug resistance, we exposed RKO cells to recombinant TGFβ in cell culture. Recombinant TGFβ increased phosphorylation of SMAD2, a sign of active TGFβ signaling, and induced a more than 100-fold increase in IC_{50} for vinorelbine (Figures S5B–S5E). To replicate the original anatomic site of colorectal cancer, we further validated our findings by orthotopic tumor implanting in mice. Two non-*BRAF*-like CC cell lines, Caco2 and HCT15 (Figures 5F and 5G) and two *BRAF*-like CC cell lines, WiDr and HCT116 (Figures 5H and 5I) were used for the generation of orthotopic engrafted tumors to measure the response to vinorelbine (see the Supplemental Experimental Procedures). As shown in Figures 5F and 5G, both Caco2 and HCT15 orthotopically implanted tumors did not respond to vinorelbine treatment, while both WiDr and HCT116 orthotopically implanted tumors significantly responded to vinorelbine (Figures 5H and 5I). Taken together, these experiments indicate that most *BRAF*-like CC tumors also have increased sensitivity to vinorelbine in vivo.

Response to Vinorelbine of Liver-Implanted Colon Cancer Cell Lines

The first site of metastatic dissemination of colon cancer is often the liver. Since new drugs are tested initially in the metastatic setting, we tested whether vinorelbine is active against colon cancer cells growing in the liver. We injected CC cells into the liver of NOD scid gamma mice and filmed them using intravital imaging upon vinorelbine treatment. We filmed the same imaging areas of CC liver implantation before, 24, and 48 hr post-vinorelbine/vehicle treatment with subcellular resolution through an abdominal imaging window as we described previously (Ritsma et al., 2012, 2013) (Figure 6A). The CC cells expressed a chimera of H2B-tagged and photo-switchable Dendra2 (H2B-Dendra2). The visualization of chromosome condensation by the fluorescent tag was used to identify mitotic status and apoptotic bodies, and the green-to-red Dendra2 photo-marking of imaging fields was used to retrace the imaging areas in subsequent imaging sessions (Figure 6A) (Janssen et al., 2013). Before treatment and during vehicle treatment (Figure S6A), only a few mitotic figures were observed in both the *BRAF*-like SNU-C5 cells and the non-*BRAF*-like Caco2 cells. Strikingly, when we imaged the same imaging field 24 hr after vinorelbine treatment, we observed a remarkable increase in mitotic figures and cell fragments in the *BRAF*-like cells implanted into the liver, but not in the non-*BRAF*-like cells growing in the liver (Figure 6B). In the next 24 hr, the number of cell fragments increased with a concomitant decrease in the number of mitotic figures (Figure 6B). These data were fully consistent with our model that *BRAF*-like cells are more sensitive to vinorelbine and that the toxicity is due to a mitotic arrest followed by apoptosis. Moreover, these data suggest that liver metastases of BRAF-like colon cancers also respond to vinorelbine therapy.

BRAF(V600E) as a Predictive Biomarker of the DM4 Response in CC PDX Models

DM4 is a potent cytotoxic agent derived from maytansine that blocks tubulin polymerization and interferes with the binding of vinblastine to tubulin, indicating a common mechanism of action (Prota et al., 2014). We therefore asked whether the sensitivity of response of CC patient-derived xenograft (PDX) to DM4 would also be predicted by BRAF mutation status. Intrinsic sensitivity to DM4 of the PDX models was determined by the antitumor efficacy of a single high dose (40 mg/kg) of a non-targeting antibody (directed against human CD19, unable to bind mouse CD19) conjugated to DM4 in tumor-bearing mice (see the Supplemental Experimental Procedures).

PDX sensitivity to the non-tumor-targeting antibody DM4 conjugate varied with 11/20 PDX models displaying lack of

(B) Boxplot of $\log_{10}$ IC_{50} values for treatment of 11 BRAF-like CC cell lines (Vaco432, WiDr, HT29, RKO, SNU-C5, KM20, OXCO-1, SW1417, SKCO-1, HCT116, and LoVo) and 11 non-*BRAF*-like CC cell lines (LIM1215, Difi, Caco2, HCA-7, HDC54, LIM1863, HCT15, SW480, SW1116, SNU1033, and HCA-46) with vinorelbine, vinblastine, and paclitaxel. Cells were treated with vinorelbine, vinblastine, or paclitaxel for 72 hr. $\log_{10}$ of IC_{50} values (nM) are shown. See Table S4.
(C–F) WT2 non-*BRAF*-like, *BRAF(V600E)*, *KRAS* mutant non-*BRAF*-like, and *KRAS* mutant *BRAF*-like CC cells were seeded at low confluence and treated with increasing concentrations of vinorelbine twice a week. Viability was assessed by a colony formation assay. Cells were fixed, stained, and photographed after 10 days of culture.
(C) WT2 non-*BRAF*-like CC cells were seeded at low confluence and treated with increasing concentrations of vinorelbine twice per week. Viability was assessed by a colony formation assay. Cells were fixed, stained, and photographed after 10 days of culture.
(D) *BRAF(V600E)* CC cells were seeded at low confluence and treated with increasing concentrations of vinorelbine twice per week. Viability was assessed by a colony formation assay. Cells were fixed, stained, and photographed after 10 days of culture.
(E) *KRAS* mutant non-*BRAF*-like CC cells were seeded at low confluence and treated with increasing concentrations of vinorelbine twice per week. Viability was assessed by a colony formation assay. Cells were fixed, stained, and photographed after 10 days of culture.
(F) *KRAS* mutant *BRAF*-like CC cells were seeded at low confluence and treated with increasing concentrations of vinorelbine twice a week. Viability was assessed by a colony formation assay. Cells were fixed, stained, and photographed after 10 days of culture.
(G and H) Vinorelbine induces mitotic arrest followed by apoptosis in *BRAF*-like CC cells. H2B-YFP WT2 CC cells (LIM1215, Caco2, and HCT15) and H2B-YFP *BRAF*-like CC cells (WiDr, RKO, and HCT116) were treated with vinorelbine (10 nM) and filmed by time-lapse microscopy over a period of 24 hr (G) and 72hr (H). Per each CC cell lines, quantification of the main phenotypes occurring upon 24 (G) or 72 hr (H) of vinorelbine treatment is reported. A minimum of 90 cells per conditions was counted.
See also Figure S4 and Table S4.

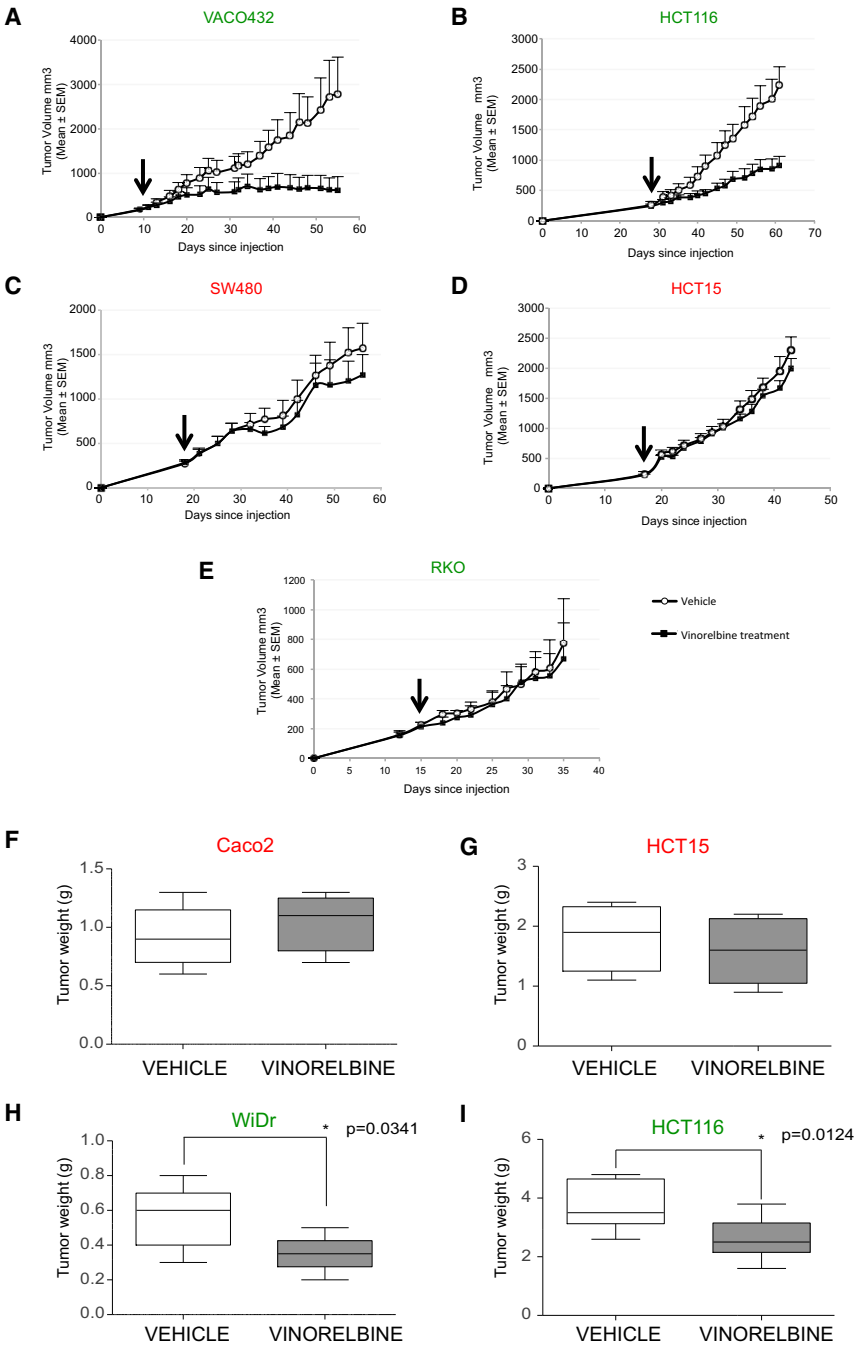

Figure 5. Vinorelbine Suppresses *BRAF*-like Tumor Growth In Vivo

(A–E) Vinorelbine can selectively suppress *BRAF*-like tumor growth in xenograft models. VACO432 cells (*BRAF*-like) (A), HCT116 cells (BRAF-like) (B), SW480 cells (non-*BRAF*-like) (C), HCT15 (non-BRAF-like) (D), and RKO cells (*BRAF*-like) (E) were grown as tumor xenografts in CD-1 nude mice. After tumor establishment (200–250 mm^3), mice were treated with either vehicle or vinorelbine (10 mg/kg intravenously [i.v.]) for the time indicated on each graph. Mean tumor volumes ± SEM (n = 5-6 mice per group). An arrow indicates initiation of treatment.

(F–I) Vinorelbine can selectively suppress BRAF-like tumor growth in orthotopic-implanted models. Caco2 (non-*BRAF*-like) (F), HCT15 (non-*BRAF*-like) (G), WiDr (*BRAF*-like) (H), and HT116 (*BRAF*-like) (I) CC cell lines were used for orthotopic implantation experiment in nude mice. Animals were treated with vehicle or vinorelbine (2.5 mg kg^{-1}) for 2 weeks. Mean tumor volumes or weights ± SEM are shown (n = 7–9 mice per group).

See also Figure S5.

Complete Remission of a BRAF-like Colon Cancer Patient with Vinca Alkaloids

A study report was published in 1994, in which 15 metastatic CC patients were treated with vinblastine in combination with bepridil to investigate if a calcium channel blocker could overcome the multi-drug resistance to vinblastine. The overall study was negative, but one out of 15 patients received complete remission that lasted over 20 years after repeated cycles of therapy with vinblastine-containing regimen (Linn et al., 1994). We retrieved the primary tumor of the patient and performed both DNA and RNA extraction to look for mutations in *KRAS*, *NRAS*, and *BRAF* genes and determine BRAF-like status by gene expression profiling. The sequence data revealed that the tumor carried a *KRAS* mutation. Gene expression analysis revealed the tumor to be BRAF-like (Figure 6D). This super-responder patient further supports the notion that BRAF-like CC are responsive to vinca alkaloids.

sensitivity and 9/20 displaying intrinsic sensitivity (Table S5). Examples of DM4-sensitive and DM4-resistant PDX models are shown in Figures S6B and S6C. Interestingly, the *BRAFV600E*-activating mutation was found exclusively in DM4-sensitive models (Figure 6C). Indeed, 44% of CC PDX responders carry the *BRAF(V600E)* mutation, while none of the non-responders carry the same BRAF-activating mutation (Fisher exact test p value = 0.026). Taken together, these data strengthen our finding of microtubules dynamic to be a specific target of BRAFV600E and eventually BRAF-like CC.

DISCUSSION

Oncogenomic studies have enabled a molecular taxonomy of colorectal cancer (Ana Sebio, 2015; Dienstmann, 2014), but to date, this has had only a limited impact on the clinical management of this disease. *BRAF(V600E)* mutations occur in about 8%–10% of CRC patients and are associated with a poor

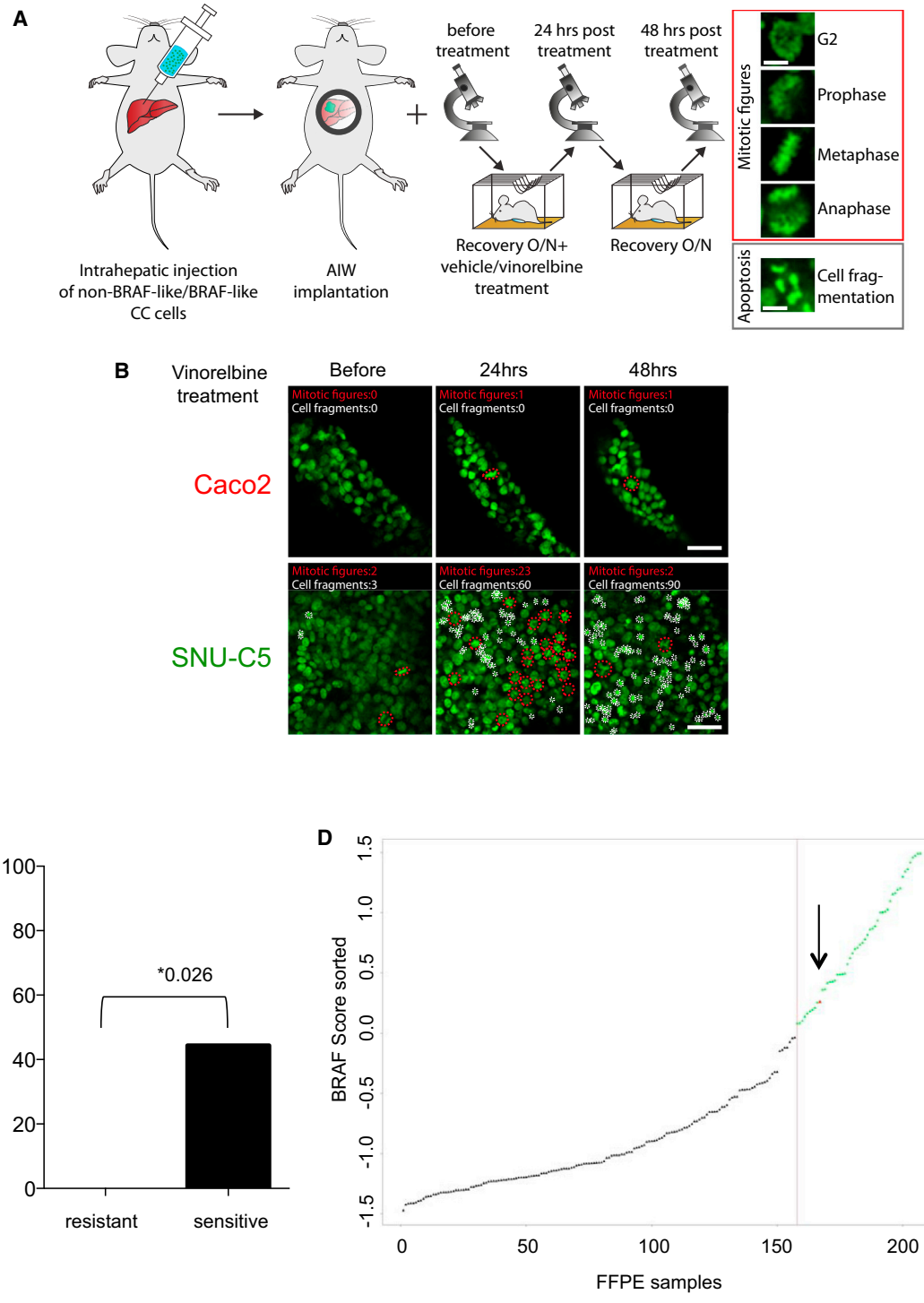

Figure 6. Vinca Alkaloids Show Significant Activity in BRAF-like CC Tumors

(A and B) Vulnerability to vinorelbine of CC cells implanted into liver revealed by intravital microscopy. (A) Cartoon showing the experimental setup. Caco2 (non-*BRAF*-like) or SNU-C5 (*BRAF*-like) CC cells labeled with H2B-Dendra2 were injected into the liver of NSG mice. Upon tumor formation, an abdominal imaging window was implanted on the liver of the recipient mice. The mice were intravitally imaged for 3 consecutive days, tracing back the same imaging areas each time point. Vehicle (PBS) or vinorelbine was administered immediately after the first imaging session. Representative examples of mitotic figures and cell fragments upon cell death were collected with intravital microscopy. Scale bar, 10 μm. (B) Intravital imaging of Caco2 (non-*BRAF*-like) and Snu-c5 (*BRAF*-like) liver tumor before, 24 hr after, and 48 hr after vinorelbine administration. The red dashed lines highlight cells undergoing mitosis. The white dashed lines indicate cell fragments. Scale bar, 50 μm.

(legend continued on next page)

prognosis, especially in the metastatic setting (Bokemeyer et al., 2011; Van Cutsem et al., 2011; Richman et al., 2009; Tol et al., 2009). These tumors can be identified by a distinctive gene expression signature. This signature reliably identifies tumors with *BRAF(V600E)* mutation and a set of tumors lacking a *BRAF* mutation. We collectively refer to the CC tumors with this *BRAF* gene signature as "*BRAF*-like." In addition to their similar gene expression profile, they are also characterized by similarly poor prognosis (Popovici et al., 2012; Tian et al., 2013). To identify additional vulnerabilities of these tumors that can be exploited therapeutically, we used a loss-of-function genetic approach. We identified *RANBP2* as an essential gene for BRAF-like CC cell lines. RANBP2 belongs to the RAS superfamily and is a major cytosolic component of filaments that derives from the cytoplasmic ring of the nuclear pore complex. More recently, RANBP2 and the RANBP2-RANGAP1 complex have been shown to play an important role in mitosis. In particular, RANBP2 has a role in the interaction of kinetochores with the microtubule bundles that extend from the centrosomes to the kinetochores (Clarke and Zhang, 2008; Joseph et al., 2004). Depletion of RANBP2 by RNAi causes defective kinetochore structure and composition, abnormal mitotic progression, and abnormal chromosome segregation (Joseph et al., 2002; Salina et al., 2003). In agreement with these reports, we observed several mitotic defects in *BRAF*-like CC cells upon *RANBP2* knockdown, in particular prolonged mitosis eventually triggering cell death. The percentage of dead cells observed during the time-lapse experiment is a function of the observation time (72 hr). Hence, the colony formation assays (performed over a 10-day period) result in more significant cell death.

The RAN-GTP gradient is important for the stabilization and nucleation of microtubules around kinetochores (Arnaoutov and Dasso, 2003). RAN-GTP binds importin-β and releases factors that are involved in spindle assembly (Clarke and Zhang, 2008), and its localization at kinetochores requires RANBP2. We found *BRAF*-like CC cell lines to be defective in the microtubule outgrowth from kinetochores and RANBP2 depletion to further reduce this microtubule outgrowth. We therefore hypothesize that RANBP2 allows BRAF-like CC cells to tolerate such a defect. Consequently, RANBP2 depletion results in cell death.

The specific defect of *BRAF*-like cells in microtubule formation unveiled a potential vulnerability of such tumors to microtubule disrupting agents. Indeed, we found that *BRAF*-like CC cells were 10- to 10,000-fold more sensitive to vinorelbine than non-*BRAF*-like CC cells. Moreover, we tested five *BRAF*-like and three non-*BRAF*-like colon cancer cells in various in vivo animal models for their sensitivity to vinorelbine. All but one cell line reacted in accordance to their gene expression profile: the *BRAF*-like being far more responsive than their non-*BRAF*-like counterparts (Figures 5 and 6). Furthermore, in a series of 20 patient-derived xenograft (PDX) models of colon cancer, we found that *BRAF(V600E)* mutation is a predictive biomarker of response to DM4, a potent anti-mitotic agent with a mechanism of action similar to vinca alkaloids.

Vinorelbine has been rarely used for the treatment of colon cancer. Only three studies have been reported (Gebbia et al., 1996; Iaffaioli et al., 1995; Linn et al., 1994). The tumor of one patient who got complete and lasting remission after vinblastine treatment could be retrieved (Linn et al., 1994). The analysis of the sample revealed the tumor to be BRAF-like by gene expression (Figure 6D). While super-responders are rare, they can point at particular biomarkers that can be used to identify patient subsets likely to benefit from specific treatment. In this particular case, the identification of this patient as BRAF-like provides an incentive to test vinorelbine in this patient group, which represents some 20% of all colon cancers. However, we cannot exclude that other factors not present in our current models will modulate clinical responses to vinorelbine. A clinical study to assess the utility of vinorelbine in *BRAF*-like colon cancer is scheduled to start in the near future. Our data also suggest that *BRAF*-like CCs are attractive subtypes to target with maytansine-derived antibody drug conjugates. More generally, our findings highlight the utility of functional genetic approaches to find vulnerabilities of subgroups of cancers that can be exploited in the clinic.

EXPERIMENTAL PROCEDURES

Selection of the Genes Used for the *BRAF*-like shRNA Library

Genes overexpressed in *BRAF(V600E)* tumors as compared to *BRAF* and *KRAS* wild-type (*WT2*) tumors from two gene expression datasets were used: Popovici et al. (2012) and Tian et al. (2013). Genes were filtered according to variability by selecting only those features for which the difference between the 95th and the 5th percentiles was greater than 0.5 log2-units. Differential expressed genes were identified with the limma package for the R statistical software (Ritchie et al., 2015). The Benjamini-Hochberg false discovery rate (FDR) was used to control for multiple hypothesis testing, with the cutoff for statistical significance set at 0.05.

Synthetic Lethal shRNA Screen

The pooled shRNA dropout screen adapted from Prahallad et al. (2012) is described in the Supplemental Experimental Procedures.

Cell Culture and Viral Transduction

Experiments were performed as described by Prahallad et al. (2012). See the Supplemental Experimental Procedures for details.

Long-Term Proliferation Assays

For the loss-of-function assays, after puromycin selection cells were seeded into six-well plates (DiFi and SKCO-1, 5 × 10^4 cells/well; all the other CC cell lines, 2 × 10^4 cells/well) and cultured for 10 days. For vinorelbine and vinblastine treatments, cells were seeded into six-well plates (DiFi, SKCO-1,

(C) BRAFV600E mutation is a discriminant of sensitivity to DM4 toxin in colon cancer PDX models. A graphical representation of the percentage of *BRAF*(V600E) PDX models within DM4 toxin-resistant and toxin-sensitive CC PDX models is shown. The y axis indicates the percentage of BRAFV600E mutant tumors within the two groups. The x axis indicates the two groups: resistant and sensitive to DM4 toxin.

(D) Complete remission of a BRAF-like metastatic CC patient upon vinblastine treatment. The BRAF FFPE scores of 207 FFPE samples are on the y axis; scores are sorted. Black indicates predicted by signature as non-BRAF-like; green indicates predicted by signature as BRAF-like; red indicates sample T14-61892; and the red line indicates the current cutoff for FFPE samples.

See also Figure S6 and Table S5.

and HDC54, 5 × 10^4 cells/well; all the other CC cell lines, 2 × 10^4 cells/well) and cultured both in the absence and presence of drugs as indicated. At the endpoints of colony formation assays, cells were fixed, stained with crystal violet, and photographed. All knockdown experiments were done by lentiviral infection. All relevant assays were performed independently at least three times. The NKI-AVL medical ethical committee approved the use of archival human tissue in this study.

Time-Lapse Microscopy and Immunofluorescence

Time-lapse experiments and immunofluorescence were adapted from Raaijmakers et al. (2009) and Tanenbaum et al. (2010). See the Supplemental Experimental Procedures for details.

SUPPLEMENTAL INFORMATION

Supplemental Information includes Supplemental Experimental Procedures, six figures, and five tables and can be found with this article online at http://dx.doi.org/10.1016/j.cell.2016.02.059.

AUTHOR CONTRIBUTIONS

L.V., V.G., S. Tejpar, and R.B. designed the screening. I.M.S., S. Tian, G.D., M.D., L.V., V.G., S. Tejpar, and R.B. generated the list of genes. R.L.B. and C.L. assisted with the screen analysis and hit selection. L.V., V.G., and R.B. designed experiments, and L.V. and V.G. performed them. J.R. and R.H.M. supervised the mitotic experiments. A.S. performed the data analysis. M.R., A. Bartolini, F.D., and A. Bardelli supervised and/or performed the xenografts experiments. A.V. and D.G.M. performed the orthotropic models experiments. A.F., E.B., and J.v.R. performed the intravital imaging. S.M. helped with the revision of the manuscript. N.E.-M., M.C., L.C., C.N., C.C., and C.H. provided the CC PDX models data. S.L. provided the patient's sample. S.i.V. and S. Tian performed the BRAF-call for the patient. L.V., V.G., and R.B. wrote the manuscript. All the authors read, revised, and approved the manuscript. R.B. supervised the work.

ACKNOWLEDGMENTS

We thank the members of the NKI Genomics Core Facility, the Pathology Department, Lauren Oomen, and Lenny Brocks from the NKI Digital Microscopy Facility for technical support. We thank the members of the IDIBELL animal core facility for the mouse care. We are grateful to Astrid Bosma, Paul van der Valk, Jan Schellens, Michiel Boekhout, Erik Voets, Roy van Heesbeen, Magali Michaut, and Rob Wolthuis for discussions and Lydia Blot, Sukhvinder Sidhu, and Véronique Blanc at Sanofi for their support. We would also like to thank John Lambert and Immunogen's colleagues for their contribution to the CC PDX work. This work was supported by grants from ESMO for Translational Research (to L.V.), an EU FP7 program grant COLTHERES (to R.B., F.D., A. Bardelli, S. Tejpar, I.M.S., S. Tian, G.D., and M.D.), an NWO grant CSBC (to R.L.B., R.B., L.W., and C.L.), the Dutch Cancer Society (KWF) (to R.B.), the Fondo de Investigaciones Sanitarias PI13-01339) and Generalitat de Catalunya (2005SGR00727) (to A.V.), AIRC IG (n. 12812) (to A. Bardelli), AIRC IG (n. 17707) (to F.N.), Fondazione Piemontese per la Ricerca sul Cancro-ONLUS 5 per mille 2010 e 2011 Ministero della Salute (to A. Bardelli and F.N.), Fondo per la Ricerca Locale (ex 60%), and Università di Torino, 2014 (to F.N.). N.E.-M., M.C., L.C., C.N., C.C., and C.H. are employees of Sanofi Oncology. I.M.S. and S. Tian were employees of Agendia at the time of the study.

Received: June 27, 2015
Revised: December 20, 2015
Accepted: February 22, 2016
Published: April 7, 2016

REFERENCES

Ana Sebio, H.-J.L. (2015). The molecular taxonomy of colorectal cancer: what's new? Curr. Colorectal Cancer Rep. *11*, 118–124.

Arnaoutov, A., and Dasso, M. (2003). The ran GTPase regulates kinetochore function. Dev. Cell *5*, 99–111.

Arnaoutov, A., Azuma, Y., Ribbeck, K., Joseph, J., Boyarchuk, Y., Karpova, T., McNally, J., and Dasso, M. (2005). Crm1 is a mitotic effector of Ran-GTP in somatic cells. Nat. Cell Biol. *7*, 626–632.

Berns, K., Horlings, H.M., Hennessy, B.T., Madiredjo, M., Hijmans, E.M., Beelen, K., Linn, S.C., Gonzalez-Angulo, A.M., Stemke-Hale, K., Hauptmann, M., et al. (2007). A functional genetic approach identifies the PI3K pathway as a major determinant of trastuzumab resistance in breast cancer. Cancer Cell *12*, 395–402.

Bokemeyer, C., Bondarenko, I., Hartmann, J.T., de Braud, F., Schuch, G., Zubel, A., Celik, I., Schlichting, M., and Koralewski, P. (2011). Efficacy according to biomarker status of cetuximab plus FOLFOX-4 as first-line treatment for metastatic colorectal cancer: the OPUS study. Ann. Oncol. *22*, 1535–1546.

Brunen, D., Willems, S.M., Kellner, U., Midgley, R., Simon, I., and Bernards, R. (2013). TGF-β: an emerging player in drug resistance. Cell Cycle *12*, 2960–2968.

Cidón, E.U. (2010). The challenge of metastatic colorectal cancer. Clin. Med. Insights Oncol. *4*, 55–60.

Clarke, P.R. (2005). The Crm de la crème of mitosis. Nat. Cell Biol. *7*, 551–552.

Clarke, P.R., and Zhang, C. (2008). Spatial and temporal coordination of mitosis by Ran GTPase. Nat. Rev. Mol. Cell Biol. *9*, 464–477.

Dienstmann, R. (2014). Colorectal Cancer Subtyping Consortium (CRCSC) identification of a consensus of molecular subtypes. J. Clin. Oncol. *32* (*Suppl*), 3511.

Garnett, M.J., Edelman, E.J., Heidorn, S.J., Greenman, C.D., Dastur, A., Lau, K.W., Greninger, P., Thompson, I.R., Luo, X., Soares, J., et al. (2012). Systematic identification of genomic markers of drug sensitivity in cancer cells. Nature *483*, 570–575.

Gebbia, V., Maiello, E., Testa, A., Cannata, G., Colucci, G., and Gebbia, N. (1996). Single agent vinorelbine in the treatment of unresectable lung metastases from colorectal cancer. Oncol. Rep. *3*, 563–565.

Glück, S., de Snoo, F., Peeters, J., Stork-Sloots, L., and Somlo, G. (2013). Molecular subtyping of early-stage breast cancer identifies a group of patients who do not benefit from neoadjuvant chemotherapy. Breast Cancer Res. Treat. *139*, 759–767.

Hashizume, C., Kobayashi, A., and Wong, R.W. (2013). Down-modulation of nucleoporin RanBP2/Nup358 impaired chromosomal alignment and induced mitotic catastrophe. Cell Death Dis. *4*, e854.

Huang, S., Hölzel, M., Knijnenburg, T., Schlicker, A., Roepman, P., McDermott, U., Garnett, M., Grernrum, W., Sun, C., Prahallad, A., et al. (2012). MED12 controls the response to multiple cancer drugs through regulation of TGF-β receptor signaling. Cell *151*, 937–950.

Iaffaioli, R., Facchini, G., Tortoriello, A., Caponigro, F., Gesue, G., Finizio, A., Dimartino, N., Desena, G., Antonelli, B., Scaramellino, G., et al. (1995). A phase-ii trial of 5-Fluorouracil, folinic Acid, vinorelbine in pretreated patients with metastic colorectal-cancer. Oncol. Rep. *2*, 513–516.

Janssen, A., Beerling, E., Medema, R., and van Rheenen, J. (2013). Intravital FRET imaging of tumor cell viability and mitosis during chemotherapy. PLoS ONE *8*, e64029.

Jemal, A., Bray, F., Center, M.M., Ferlay, J., Ward, E., and Forman, D. (2011). Global cancer statistics. CA Cancer J. Clin. *61*, 69–90.

Joseph, J., Tan, S.H., Karpova, T.S., McNally, J.G., and Dasso, M. (2002). SUMO-1 targets RanGAP1 to kinetochores and mitotic spindles. J. Cell Biol. *156*, 595–602.

Joseph, J., Liu, S.T., Jablonski, S.A., Yen, T.J., and Dasso, M. (2004). The RanGAP1-RanBP2 complex is essential for microtubule-kinetochore interactions in vivo. Curr. Biol. *14*, 611–617.

Linn, S.C., Giaccone, G., and Pinedo, H.M. (1994). Complete remission of metastatic colorectal cancer: a pitfall in a multidrug resistance reversal trial. Lancet *343*, 1648–1649.

Luo, J., Emanuele, M.J., Li, D., Creighton, C.J., Schlabach, M.R., Westbrook, T.F., Wong, K.K., and Elledge, S.J. (2009). A genome-wide RNAi screen identifies multiple synthetic lethal interactions with the Ras oncogene. Cell *137*, 835–848.

Popovici, V., Budinska, E., Tejpar, S., Weinrich, S., Estrella, H., Hodgson, G., Van Cutsem, E., Xie, T., Bosman, F.T., Roth, A.D., and Delorenzi, M. (2012). Identification of a poor-prognosis BRAF-mutant-like population of patients with colon cancer. J. Clin. Oncol. *30*, 1288–1295.

Prahallad, A., Sun, C., Huang, S., Di Nicolantonio, F., Salazar, R., Zecchin, D., Beijersbergen, R.L., Bardelli, A., and Bernards, R. (2012). Unresponsiveness of colon cancer to BRAF(V600E) inhibition through feedback activation of EGFR. Nature *483*, 100–103.

Prota, A.E., Bargsten, K., Diaz, J.F., Marsh, M., Cuevas, C., Liniger, M., Neuhaus, C., Andreu, J.M., Altmann, K.-H., and Steinmetz, M.O. (2014). A new tubulin-binding site and pharmacophore for microtubule-destabilizing anticancer drugs. Proc. Natl. Acad. Sci. USA *111*, 13817–13821.

Raaijmakers, J.A., Tanenbaum, M.E., Maia, A.F., and Medema, R.H. (2009). RAMA1 is a novel kinetochore protein involved in kinetochore-microtubule attachment. J. Cell Sci. *122*, 2436–2445.

Richman, S.D., Seymour, M.T., Chambers, P., Elliott, F., Daly, C.L., Meade, A.M., Taylor, G., Barrett, J.H., and Quirke, P. (2009). KRAS and BRAF mutations in advanced colorectal cancer are associated with poor prognosis but do not preclude benefit from oxaliplatin or irinotecan: results from the MRC FOCUS trial. J. Clin. Oncol. *27*, 5931–5937.

Ritchie, M.E., Phipson, B., Wu, D., Hu, Y., Law, C.W., Shi, W., and Smyth, G.K. (2015). limma powers differential expression analyses for RNA-sequencing and microarray studies. Nucleic Acids Res. *43*, e47.

Ritsma, L., Steller, E.J. a., Beerling, E., Loomans, C.J.M., Zomer, A., Gerlach, C., Vrisekoop, N., Seinstra, D., van Gurp, L., Schafer, R., et al. (2012). Intravital microscopy through an abdominal imaging window reveals a pre-micrometastasis stage during liver metastasis. Sci. Transl. Med. *4*, 158ra145.

Ritsma, L., Steller, E.J., Ellenbroek, S.I., Kranenburg, O., Borel Rinkes, I.H., and van Rheenen, J. (2013). Surgical implantation of an abdominal imaging window for intravital microscopy. Nat. Protoc. *8*, 583–594.

Roepman, P., Schlicker, A., Tabernero, J., Majewski, I., Tian, S., Moreno, V., Snel, M.H., Chresta, C.M., Rosenberg, R., Nitsche, U., et al. (2014). Colorectal cancer intrinsic subtypes predict chemotherapy benefit, deficient mismatch repair and epithelial-to-mesenchymal transition. Int. J. Cancer *134*, 552–562.

Salina, D., Enarson, P., Rattner, J.B., and Burke, B. (2003). Nup358 integrates nuclear envelope breakdown with kinetochore assembly. J. Cell Biol. *162*, 991–1001.

Sargent, D.J. (2014). Prognostic impact of deficient mismatch repair (dMMR) in 7,803 stage II/III colon cancer (CC) patients (pts): a pooled individual pt data analysis of 17 adjuvant trials in the ACCENT database. J. Clin. Oncol. *32* (*Suppl*), 3507.

Sinicrope, F.A., Foster, N.R., Thibodeau, S.N., Marsoni, S., Monges, G., Labianca, R., Kim, G.P., Yothers, G., Allegra, C., Moore, M.J., et al. (2011). DNA mismatch repair status and colon cancer recurrence and survival in clinical trials of 5-fluorouracil-based adjuvant therapy. J. Natl. Cancer Inst. *103*, 863–875.

Steckel, M., Molina-Arcas, M., Weigelt, B., Marani, M., Warne, P.H., Kuznetsov, H., Kelly, G., Saunders, B., Howell, M., Downward, J., and Hancock, D.C. (2012). Determination of synthetic lethal interactions in KRAS oncogene-dependent cancer cells reveals novel therapeutic targeting strategies. Cell Res. *22*, 1227–1245.

Tanenbaum, M.E., Vallenius, T., Geers, E.F., Greene, L., Mäkelä, T.P., and Medema, R.H. (2010). Cyclin G-associated kinase promotes microtubule outgrowth from chromosomes during spindle assembly. Chromosoma *119*, 415–424.

Tian, S., Simon, I., Moreno, V., Roepman, P., Tabernero, J., Snel, M., van't Veer, L., Salazar, R., Bernards, R., and Capella, G. (2013). A combined oncogenic pathway signature of BRAF, KRAS and PI3KCA mutation improves colorectal cancer classification and cetuximab treatment prediction. Gut *62*, 540–549.

Tie, J., Gibbs, P., Lipton, L., Christie, M., Jorissen, R.N., Burgess, A.W., Croxford, M., Jones, I., Langland, R., Kosmider, S., et al. (2011). Optimizing targeted therapeutic development: analysis of a colorectal cancer patient population with the BRAF(V600E) mutation. Int. J. Cancer *128*, 2075–2084.

Tol, J., Nagtegaal, I.D., and Punt, C.J. (2009). BRAF mutation in metastatic colorectal cancer. N. Engl. J. Med. *361*, 98–99.

Torosantucci, L., De Luca, M., Guarguaglini, G., Lavia, P., and Degrassi, F. (2008). Localized RanGTP accumulation promotes microtubule nucleation at kinetochores in somatic mammalian cells. Mol. Biol. Cell *19*, 1873–1882.

Van Cutsem, E., Köhne, C.-H., Láng, I., Folprecht, G., Nowacki, M.P., Cascinu, S., Shchepotin, I., Maurel, J., Cunningham, D., Tejpar, S., et al. (2011). Cetuximab plus irinotecan, fluorouracil, and leucovorin as first-line treatment for metastatic colorectal cancer: updated analysis of overall survival according to tumor KRAS and BRAF mutation status. J. Clin. Oncol. *29*, 2011–2019.

Vollebergh, M.A., Lips, E.H., Nederlof, P.M., Wessels, L.F., Wesseling, J., Vd Vijver, M.J., de Vries, E.G., van Tinteren, H., Jonkers, J., Hauptmann, M., et al. (2014). Genomic patterns resembling BRCA1- and BRCA2-mutated breast cancers predict benefit of intensified carboplatin-based chemotherapy. Breast Cancer Res. *16*, R47.

Yuan, Z.-X., Wang, X.-Y., Qin, Q.-Y., Chen, D.-F., Zhong, Q.-H., Wang, L., and Wang, J.-P. (2013). The prognostic role of BRAF mutation in metastatic colorectal cancer receiving anti-EGFR monoclonal antibodies: a meta-analysis. PLoS ONE *8*, e65995.